ELSEVIER

Biophysical Chemistry 84 (2000) 269–279

Biophysical Chemistry

www.elsevier.nl/locate/bpc

Compared effects of cholesterol and 7-dehydrocholesterol on sphingomyelin–glycerophospholipid bilayers studied by ESR

Claude Wolf*, Claude Chachaty

Service de Biochimie, Laboratoire Commun de Spectrométrie, INSERM U538, Faculté de Médecine de Saint-Antoine, 27 rue Chaligny, 75571 Paris Cedex 12, France

Received 5 August 1999; received in revised form 24 February 2000; accepted 7 March 2000

Abstract

The ESR of 7- and 16-doxylstearic spin-labeled fatty acids (7NS and 16NS, respectively) reveal the distinct influence of cholesterol or cholesterol precursor analogue, Δ7-dehydrocholesterol, on the molecular ordering and the fluidity of lipid mixtures containing sphingomyelin (SM). The phase-separation of sphingomyelin domains mixed within fluid glycerophospholipids (phosphatidylethanolamine and phosphatidylserine) can be followed by ESR as a function of the temperature and in the presence of sterols [cholesterol (CHOL) or 7-dehydrocholesterol (DHCHOL)]. The time scale of spin-label exchange among phases is appropriate to follow the occurrence of the specific sphingomyelin/sterol association forming liquid ordered (Lo) microdomains which separate from the fluid surrounding phase Lα. Sphingomyelin embedded within the fluid bilayer associates with both sterols below 36°C to give a phase Lo traceable by ESR in the form of a highly anisotropic component. Above 36°C, the contribution in the ESR spectrum, of the Lo phase formed by 7-dehydrocholesterol with sphingomyelin is reduced by contrast with cholesterol forming a temperature-stable liquid ordered phase up to 42°C. The consequences of this destabilization of the SM/sterol microdomains are envisioned in the biosynthesis defect where the precursor 7-dehydrocholesterol substitutes, for a significant part, the embryonic cell cholesterol.

Keywords: Cholesterol; 7-Dehydrocholesterol; Sphingomyelin; Membrane microdomains; Lo/Lα phase-separation; ESR spectral simulations; Smith–Lemli–Opitz syndrome

Abbreviations: 7NS and 16NS, 7- and 16-doxylstearic spin-labeled fatty acids; SM, Sphingomyelin; PE, Phosphatidylethanolamine; PS, Phosphatidylserine; GPL, Glycero-phospholipids; CHOL, Cholesterol; DHCHOL, 7-dehydrocholesterol; Lo, Liquid ordered lamellar phase; Lα, Fluid liquid crystalline lamellar phase

* Corresponding author. Tel.: +33-1400-113-47; fax: +33-1400-114-99.
E-mail address: wolf@ccr.jussieu.fr (C. Wolf)

0301-4622/00/$ - see front matter
PII: S0301-4622(00)00135-6

1. Introduction

The structural and visco-dynamic properties of phospholipid and cholesterol assemblies are relevant to a number of biological studies where membranes play a decisive role. Such information needs to be approached by spectroscopic methods like ESR in complement with X-ray diffraction which provides the structure of the liquid-crystalline phases. This holds especially for short life-time microdomains suspected to occur at physiological temperatures within lipid mixtures comprising the so-called 'liquid-ordered (Lo)' phase formed by cholesterol/sphingomyelin [1]. The possible short life-time of these domains justifies the study by CW X-band ESR which provides information in the 10–1000 ns time scale for a probe exchanging among phases.

An X-ray diffraction study in progress shows that sphingomyelin (SM) suppresses the heterogeneity of a binary mixture comprising the inverted hexagonal phase (H_{II}) formed by PE which coexists with the lamellar arrangement formed by PS. The strong phase preference exerted by added SM stabilizes a lamellar arrangement for the ternary mixture of PE/PS/SM (aminoglycerophospholipids/SM: 7/3: mole/mole) around the physiological temperature. While sphingolipids form gel-separated domains within fluid-phase bilayers, the effect of sterol addition on the stability and size of the sphingolipid-enriched domains remains questionable [2]. In the present study, the influence of SM after addition of a sterol has been examined with the goal of observing the phase separation of a sterol/SM association from the fluid glycerophospholipids.

The present physical study of 7-dehydrocholesterol (DHCHOL) compared with cholesterol is related to the deficit of membrane microdomains where a blockade of the cholesterol synthesis occurs under pathological conditions. Such a deficit in the supply of endogenous cholesterol is encountered in embryos affected by the Smith–Lemli–Opitz (SLO) malformations syndrome [3]. The synthesis of cholesterol being blocked at the 7-dehydrocholesterol reductase step in SLO, the embryo cholesterol is decreased during the early embryogenesis and the precursor accumulates. This condition results, in turn, in the deficit of the expression of a development patterning protein called 'Sonic Hedgehog' which requires membrane cholesterol for its maturation. The deficit in sterol-rich microdomains with consequences on the Sonic Hedgehog processing has been recently illustrated by Rietveld et al. [4] in *Drosophila*. The correlation between the lack of cholesterol with the malformations of knocked-out embryos for Sonic Hedgehog is also found in the offspring from pregnant dams treated by the distal cholesterol inhibitor AY9944. The malformations are suppressed by an abundant dietary cholesterol to the dams [5].

The present studies is aimed to understand why the close analog precursor (DHCHOL has two conjugated Δ5,7 double bonds in the B-ring but CHOL has a unique Δ5 double bond) cannot form the microdomains where proteins such as Sonic Hedgehog can be docked. The SM/CHOL interaction has previously focused much interest [6–9] but a critical discrimination between different sterols to form the 'rafts' requires complementary studies due to their variety [10]. The temperatures to conduct the observations are also critical: the observation of ergosterol influence in *Drosophila* are meaningful at room temperature [4], whereas for cholesterol in human or rat, temperatures of approximately 37°C are significant. The present study has been performed with lipids of biological extraction including a sphingomyelin from egg yolk comprising 75% of palmitic acid which forms gel-state lamellae above the physiological temperature. The phase-separation of gel sphingomyelin within fluid polyunsaturated glycerophospholipids is suppressed by CHOL and DHCHOL. The efficiencies of CHOL and DHCHOL are compared for the emergence of Lo microdomains. The difference between sterols to stabilize the microdomains is examined by ESR with regard to its relevance to pathology.

2. Methods

2.1. Experimental procedures

The lipids (egg yolk SM, beef brain PS, egg yolk

PE, CHOL and DHCHOL) and the spin-labeled fatty acids have been provided by Sigma (Sigma-Aldrich Chimie SARL, 38297 St Quentin, France). Lipid mixtures of the appropriate composition are prepared from chloroform solutions, vacuum-dried for 24 h and hydrated in excess purified water above 40°C. The spin label is added as an aliquot of a concentrated ethanol solution (10^{-2} M) and the sample is equilibrated before the measurement. The equilibration process is followed by the disappearance of the narrow lines of the spin label not incorporated in the vesicles which is completed within 1 day at room temperature.

The ESR spectra of 7NS and 16NS have been recorded between 32 and 42°C, i.e. in a 10°C range where the various biological molecular species of SM undergo the gel-to-fluid transition. The ESR spectra have been performed with a Bruker ER200D X-band spectrometer (Bruker Spectrospin, Wissembourg) equipped with a variable temperature device and a digital signal recording (EPR Ware, Scientific Software Services, Bloomington, IL, USA).

Non-crystalline X-ray diffractograms have been obtained at station 8.2 of the Daresbury Laboratory Synchrotron facility (UK) as a function of the temperature [11]. The complete study comprising the simultaneous wide-angle and small-angle scattering will be reported elsewhere.

2.2. Spectral simulations

Three sets of parameters are extracted from spectral simulations of nitroxide spin-probes in lamellar lyotropic mesophases formed from phospholipids:

1. The order parameters defining the *ensemble-average* orientations of the X, Y and Z principal axes common to the nitrogen hyperfine coupling tensor **A** and to the **g** tensor with respect to the local director Δ_L. Here, the order parameter of major concern is:

$$\bar{P}_2(\cos\theta) = \frac{1}{2}\langle 3\cos^2\theta - 1\rangle \qquad (1)$$

denoted hereafter as $\bar{P}_2$, θ being the time-dependent angle between Δ_L and the axis of the nitrogen centered $2p_z$ orbital.

2. The effective correlation time τ of the motion of the Z-axis which for doxylstearic spin probes may be assumed to be on the average, parallel to the mean axis Δ_M of the stearoyl chain.

3. The nitrogen hyperfine coupling constant a_N which depends on the local polarity [12,13], increasing from 1.3–1.4 mT in non-polar solvents to 1.7 mT in water.

As pointed out by McConnell [14], there is an important distinction between the *ensemble-average* order parameter $\bar{P}_2$, and the *frequency-amplitude* order parameter S^*. The latter is observed even in isotropic medium, when the motion is too slow to achieve a complete averaging of magnetic tensors. In lamellar phases, the observed order parameter $S_{obs} \cong \dfrac{a_{\parallel} - a_{\perp}}{a_{zz} - (1/2)(a_{xx} + a_{yy})}$ is the sum of $\bar{P}_2$ and S^* which depend on the molecular order and on the rate of reorientation of the probe, respectively, a_{xx}, a_{yy} and a_{zz} being the principal components of the hyperfine coupling tensor and $a_{\parallel}$, $a_{\perp}$ their averaged values. The frontier between the fast and slow motional regimes where $S_{obs} = \bar{P}_2$ and $S_{obs} = \bar{P}_2 + S^*$, respectively, is approximately $\tau = [(1 - \bar{P}_2)\Delta A]^{-1}$, $\Delta A = \gamma_e[a_{zz} - (1/2)(a_{xx} + a_{yy})]$ being the anisotropy of the hyperfine coupling in s^{-1} and γ_e is the electron magnetogyric ratio. For a nitroxide radical at X-band frequencies, τ is of the order of 1–2 ns. S^* may be estimated by means of the diagram represented on Fig. 1 where the dependence of S_{obs} upon τ for several values of $\bar{P}_2$ between 0 and 0.6 is obtained from spectral simulations using the MOMDL program of Freed et al. [15,16].

In the fast motional regime for isotropic or anisotropic media, the homogeneous Lorentzian linewidths at half-height are given by:

$$\Delta B(M_I) = [\gamma_e T_2(M_I)]^{-1} = a + bM_I + cM_I^2 \qquad (2)$$

where M_I is the nuclear magnetic quantum number, and a, b and c are constants dependent on the intensity of the magnetic field, of the anisotropy of the **A** and **g** tensors and on the

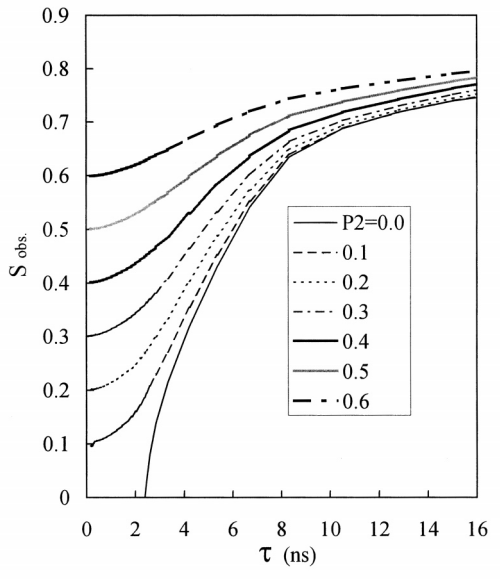

Fig. 1. Dependence of the observed order parameter S_{obs} on the effective correlation time τ for several values of the 'true' *ensemble-average* order parameter $\bar{P}_2$. Note the convergence of S_{obs} as τ increases in the slow-motional regime.

reorientation correlation times [17]. In liquid crystals these constants are also functions of the order parameter $\bar{P}_2$ and depend on the angle Θ of the local director Δ_L with respect to the magnetic field [18].

There is a possible contribution ΔB_L of dipolar or exchange electron–electron spin interactions to the Lorentzian linewidths, independent of M_I. The additional inhomogeneous broadening mainly due to unresolved hyperfine couplings is taken into account by convolution of the spectrum by a Gaussian of standard deviation ΔB_G. The spectra of randomly oriented samples are simulated by a weighted sum of spectra computed for each value of Θ, increasing by 1–3° steps from 0 to 90°.

The experimental spectra have been fitted taking as adjustable parameters $\bar{P}_2$, τ, a_N, ΔB_L, ΔB_G and the value B_0 of the magnetic field for $g = 2.00232$. For the doxyl radicals, we have taken from Jost et al. [19] $g_{xx} = 2.0088$, $g_{yy} = 2.0058$, $g_{zz} = 2.0022$ and $a_{xx} = 0.59$, $a_{yy} = 0.54$, $a_{zz} = 3.3$ mT. These principal values of the **A** tensor giving a mean value of 1.47 mT have been corrected by a factor $a_N/1.47$, a_N being the hyperfine coupling constant derived from spectral simulations. In this study, the optimization of the adjustable parameters was performed by minimizing the least-squares of the difference between the experimental and simulated spectra using the Levenberg–Marquardt algorithm [20], as reported by Chachaty and Soulié [21].

The spectra appearing as in Fig. 2a as the sum of two exchange-broadened components have been simulated by means of Bloch's equations modified for an exchange between two sites [22,23] denoted **1** and **2**. Here the exchange occurs between a quasi-isotropic ($\bar{P}_2 < 0.05$) and an anisotropic site. The adjustable parameters of major importance are the order parameter of the anisotropic site, the effective correlation time for each site, the molecular fraction F_1 of the probe in one of them and the exchange rate defined as:

$$\nu_{ex} = F_1 K_{12} = (1 - F_1) K_{21} \tag{3}$$

K_{12} and K_{21} being the probabilities per unit time of transfer of the probe from site **1** to **2** and from site **2** to **1**. The other adjustable parameters are ΔB_L, ΔB_G and a_N, assumed to be the same for the two sites.

Test simulations show that in the present case the exchange is not detected below $\nu_{ex} \sim 10^6$ s^{-1} and that the collapse of the two components occurs between 2×10^7 and 10^8 s^{-1} according to the proportion of the components and to the difference between the residual anisotropic hyperfine couplings of the probe in sites **1** and **2**:

$$\Delta A_{12} = |S_{obs1} - S_{obs2}|\, \gamma_e \left[a_{zz} - (1/2)(a_{xx} + a_{yy}) \right] \tag{4}$$

The slow, intermediate and fast exchange regimes correspond to $\nu_{ex} < \Delta A_{12}$, $\nu_{ex} \cong \Delta A_{12}$ and $\nu_{ex} > \Delta A_{12}$, respectively. As $|S_{obs1} - S_{obs2}|$ decreases when τ increases (Fig. 1), one can pass from the slow to the fast exchange regime by slowing down the reorientation of the probe on both sites.

The programs of automated fitting of spectra relevant to the fast motional regime and to the two-sites exchange have been written in APL (Array Processing Language) as reported in [21]

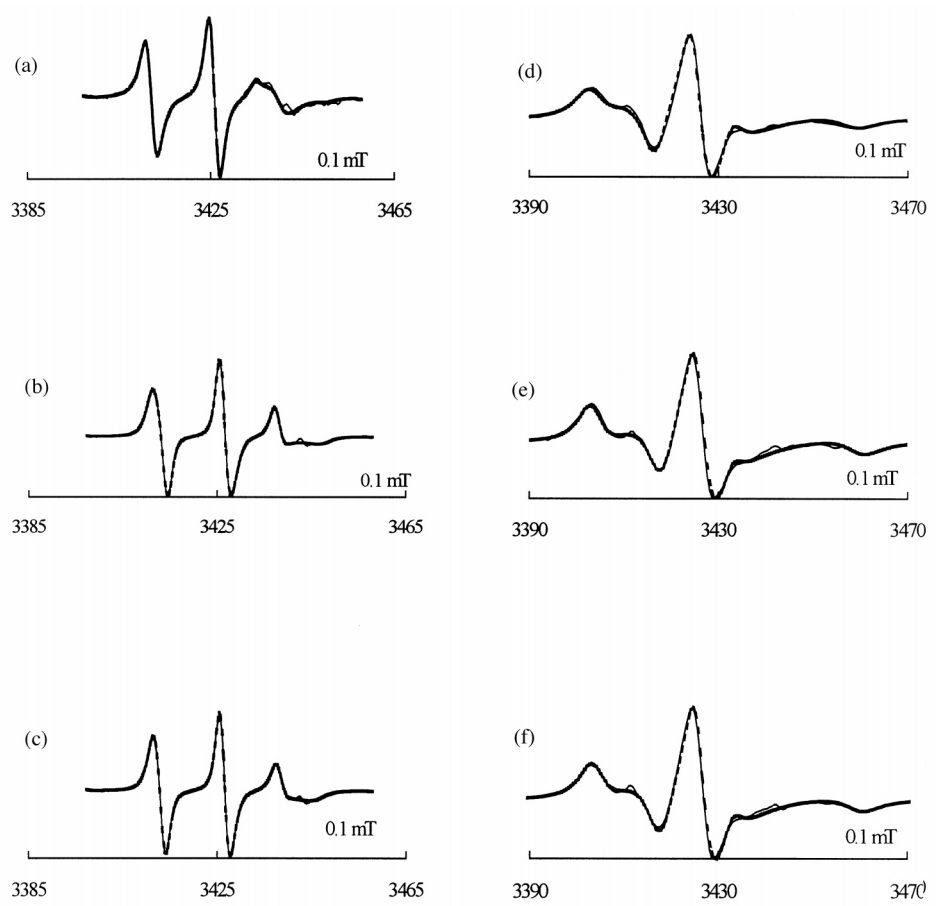

Fig. 2. Experimental (solid lines) and computed (dashed lines) spectra of doxylstearic spin-probes 16NS (left column) and 7NS (right column) at 37°C in: (a,d) sphingomyelin/phosphatidylethanolamine/phosphatidylserine (2/4/1: mole/mole); (b,e) SM/PE/PS/CHOL (2/4/1/2: mole/mole); and (c,f) SM/PE/PS/DHCHOL (2/4/1/2: mole/mole). The order parameters and reorientation correlation times used in the simulations are given in Table 1.

and are available from claude.chachaty@wanadoo.fr. These programs have been applied to the 16NS probe but not to 7NS whose spectra are relevant to the slow motional regime. In this case, we have used a version for PC of the MOMDL program of Freed et al. [15,16] which allows the simulation of spectra for randomly oriented liquid crystalline samples. For the simulation of spectra of the 7NS probe we have proceeded by the following steps:

1. Preliminary automated fitting of the spectra to determine the principal values of the averaged **A** and **g** tensors, yielding S_{obs} and a_N.
2. Calculation by the MOMDL program of a set of spectra without inhomogeneous broadening, for several values of $\bar{P}_2$ and τ yielding anisotropies of magnetic tensors **A** and **g** equal to those determined in step 1.
3. Fitting of the experimental spectrum using the set of spectra calculated in step 2 taking the ΔB_L and ΔB_G linewidths as automatically adjusted parameters. The values sought for $\bar{P}_2$ and τ correspond to the computed spectrum giving the minimum standard deviation with the experimental one. Fig. 1 shows that the values of S_{obs} for different $\bar{P}_2$ converge when τ increases in the slow motional

regime. However, the shapes of spectral components remain quite dependent on $\bar{P}_2$ and τ, ensuring a reliable determination of these parameters at least up to $\tau = 15$ ns.

3. Results

In the ternary mixture (SM/PE/PS), the 16NS spectrum (Fig. 2a) is significant of an exchange of the probe between quasi-isotropic and ordered sites. The fraction of the quasi-isotropic component derived from automatic fitting as indicated in Section 2 increases smoothly from 0.65 to 0.78 between 32 and 44°C. This fraction corresponds approximately to the molar ratio (0.7) of the polyunsaturated fluid glycerophospholipid fraction (PE and PS) indicating that the spin-probe 16NS has partitioned with the same affinity in the fluid- (GPL) and the gel-state lipids (SM). The wide-angle X-ray reflection observed at 10° in the WAXS diagram in Fig. 3 confirms the occurrence of a well-ordered and phase-separated gel arrangement of SM saturated chains. This arrangement is detected within the lamellae comprising the ternary mixture of PE/PS/SM which exhibits a repeat distance of 6.19 nm at 37°C on the SAXS diagram (Fig. 3). The gel reflection is traceable up to 39°C, which establishes the existence of the gel SM at 37°C.

No such heterogeneity is observed in the ESR spectra of 7NS (Fig. 2, right column). The reporter group being located at a more shallow more ordered depth than the center of the bilayer probed by 16NS, 7NS experiences the slow motional regime where the residual anisotropy of the hyperfine coupling proportional to S_{obs} becomes less and less dependent on $\bar{P}_2$ as τ increases (see Fig. 1). As a consequence the difference ΔA_{12} between the anisotropies of the hyperfine coupling of ordered and poorly ordered domains [Eq. (4)] may be reduced to less than the exchange rate as pointed out in Section 2. In such condi-

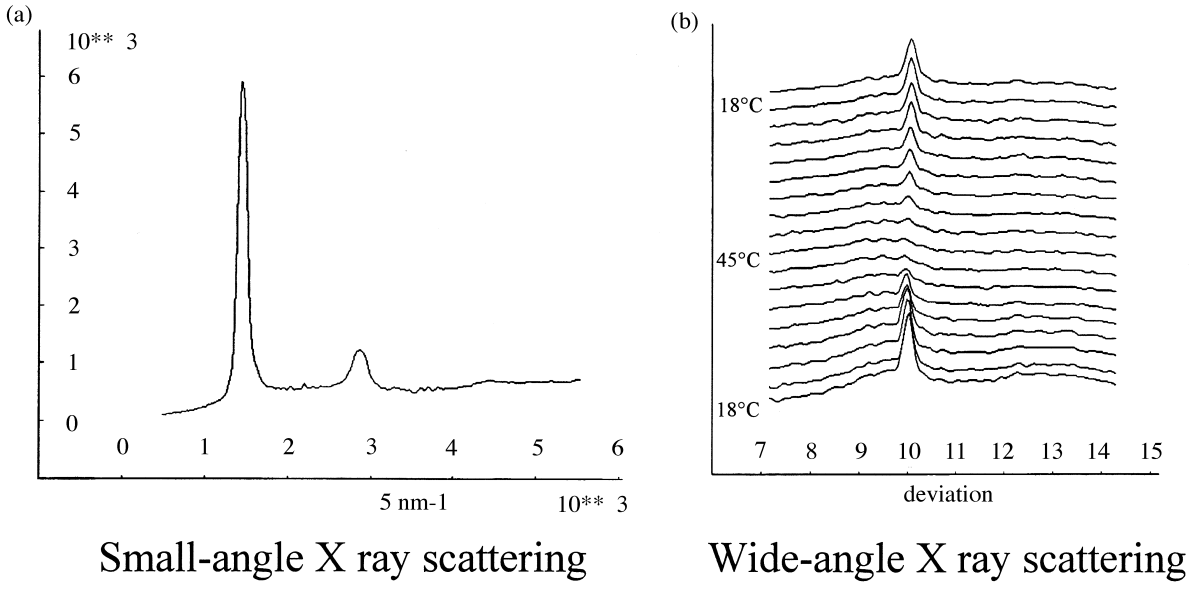

Fig. 3. Wide- (WAXS) and small-angle (SAXS) X-ray scattering by the ternary mixture sphingomyelin/phosphatidylethanolamine/phosphatidylserine (2/4/1: mole/mole). SAXS at 37°C indicates a prominent lamellar arrangement with a periodicity of 6.19 nm. WAXS points out the gel arrangement of the acyl chains with a short periodicity of 0.41 nm. This gel arrangement corresponding to an angle of 10° disappears reversibly on the diffractogram over 39°C. WAXS displays the successive recordings during a temperature cycle 18–45–18°C at 1.5°C/min.

Table 1
Order parameters, correlation times, exchange rates and nitrogen hyperfine coupling constants

	$\bar{P}_2$	τ (ns)		Isotropic ↔ anisotropic exchange rate (s^{-1})		a_N (mT)
T (°C)	37	32	42	32	42	32–42
Probe/sample						
16NS/SM + GPL:				6.2×10^6	1.0×10^7	1.39 ± 0.01
Isotropic component	–	1.4	1.1			
Anisotropic component	0.40	0.9	0.75			
16NS/SM + GPL + CHOL	0.27	0.45	0.45			1.40 ± 0.01
16NS/SM + GPL + DCHOL	0.23	0.5	0.5			1.40 ± 0.01
7NS/SM + GPL	0.25	7.2	6.6			1.56 ± 0.01
7NS/SM + GPL + CHOL	0.44	9.3	7.6			1.52 ± 0.01
7NS/SM + GPL + DCHOL	0.42	8.8	7.4			1.52 ± 0.01

tions where the fast exchange holds, a single component spectrum is observed and the $\bar{P}_2$ value derived from spectral simulation is a weighted average between the two sites. This is actually the case since for an ordered homogeneous anisotropic phase, the order parameter should be significantly larger for 7NS close to the phospholipid head group than for 16NS, whereas Table 1 shows the opposite: the $\bar{P}_2$ value (0.27) of 7NS is below that of the 16NS anisotropic component (0.40).

The spectra of 16NS and 7NS in samples containing CHOL or DHCHOL show a single anisotropic component in the overall temperature range investigated. In the absence of sterols, the weight-averaged order parameter taking into account the fraction of the isotropic and anisotropic components of 16NS derived from automated fitting (see Section 2) is $\bar{P}_2 \approx 0.1$ against $\bar{P}_2 \approx 0.25$ upon sterol addition. This increase reflects the strong organizing effect of both sterols within the deepest part of the fluid glycerophospholipid (GPL) bilayers probed by 16NS, which constitutes the major component of the ternary mixture PE/PS/SM. Noticeably, the sterols display a disordering influence on the gel SM and an ordering influence on the fluid GPL as judged by the 16NS probing the central part of the lamellae. Only a 15–20% higher ordering effect of CHOL as compared with DHCHOL is detected by 16NS in the sample containing GPL (Fig. 4) whereas we did not observe any difference for pure SM.

More significant differences between the sterols can be seen with 7NS, especially at temperatures above the gel-to-fluid transition of SM. CHOL increases the order parameter of 7NS in pure SM in the whole temperature range but DHCHOL loses this ordering influence above 35°C (Fig. 5). Fig. 6 illustrates more clearly the distinction between CHOL and DHCHOL at temperatures above 37°C in the ternary mixture PE/PS/SM. Whereas CHOL keeps a high $\bar{P}_2$ value (> 0.4) of the lipid mixture, the DHCHOL-containing sample loses rapidly the molecular order. As discussed below, these data are in agreement with the different partitioning of CHOL and DHCHOL in SM-enriched domains above the physiological temperature. The association of CHOL with SM is maintained to form stable domains whereas the association of DHCHOL is considerably weakened. It is remarkable that the ability of both sterols to form the liquid ordered phase with SM is similar at low temperatures whereas it is clearly distinct above 35°C (Fig. 6 and Table 1).

No significant effect on the nitrogen coupling constant a_N of 16NS deeply embedded in the hydrocarbon core is observed upon sterol addition, but CHOL and DHCHOL reduce a_N from 1.56 to 1.52 mT (Table 1). This reflects the reduction of the polarity (hydration) at the vicinity of the reporter group and is correlated to the increased order parameter $\bar{P}_2$ involving a higher *trans* rotamer probability for the acyl chains [24] which moves away the reporter group from the water interface.

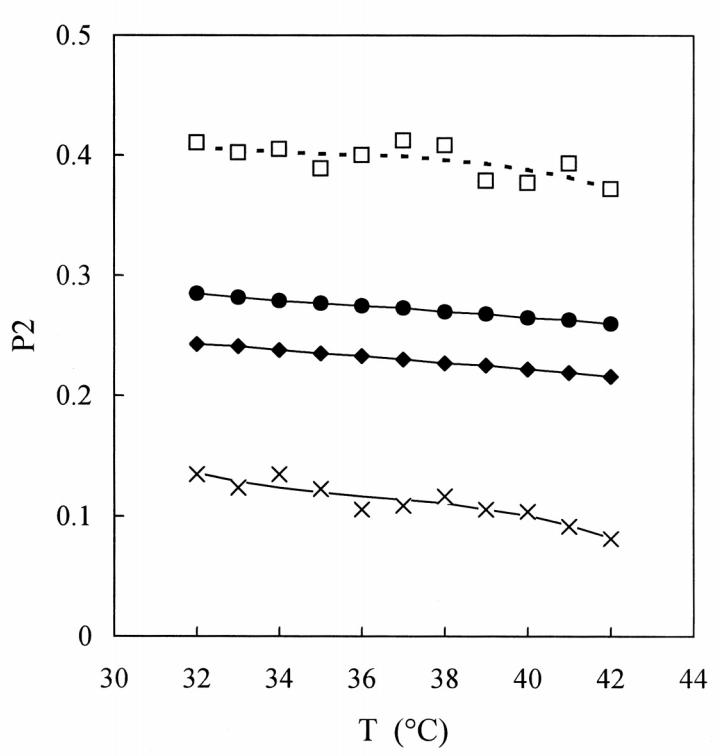

Fig. 4. Influence of the temperature on the order parameter $\bar{P}_2$ of 16NS in SM/PE/PS (2/4/1: mole/mole): (□) anisotropic component calculated from the spectral simulation; (×) weighted-average of the isotropic and anisotropic components, calculated from their respective contribution derived from spectral simulation (see Section 2); (●) SM/PE/PS/CHOL (2/4/1/2:mole/mole); (♦) SM/PE/PS/DHCHOL (2/4/1/2: mole/mole).

4. Discussion and conclusion

Simulation of ESR spectra provide details on the heterogeneity of model membrane comprising fluid and gel phospholipids which was only roughly detected by an empirical indicator such as the outer hyperfine splitting A_{max} [25]. A similar phase-separation is suspected also in biological membranes where sphingolipids (SM, glycolipids and ceramides) undergo a gel-to-fluid transition well above the physiological temperature whereas polyunsaturated glycerophospholipids form a surrounding fluid matrix. The question is whether such a heterogeneity can effectively take place in the biological membranes despite that the cholesterol smears out the differences of fluidity and molecular order between phospholipids.

The fluid *continuum* model of the biological membrane is in disagreement with the preferential interaction of CHOL with sphingolipid, which forms the so-called liquid-ordered phase, Lo, separated from the fluid (disordered) phase, Lα [26]. The Lo stability results of the multiple van der Waals bonds between the smooth α-face of the sterol ring and the stiff saturated acyl chains at a temperature below the gel-to-fluid transition of SM [27]. Hydrogen-bonding of the sterol 3-β hydroxyl with the amide group has also been considered [28]. The resistance of such tightly packed cholesterol-sphingolipid domains to Triton X100 at 4°C (producing the so-called 'detergent resistant membranes' or 'rafts' isolated from biological membranes) suggests the view that the association exists also at physiological temperatures [29]. In addition, the association to the liquid-ordered domains with proteins (including caveolins, GPI-

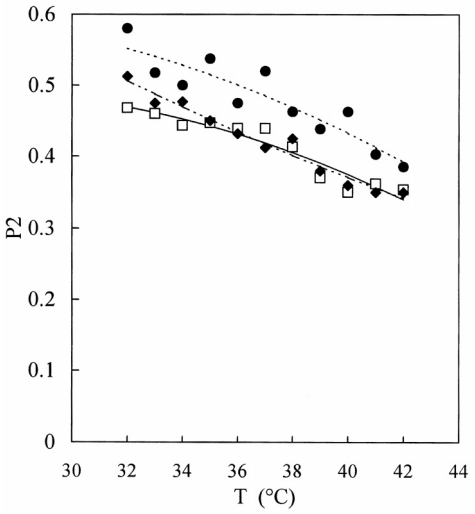

Fig. 5. Temperature dependence of the order parameter of the spin labeled fatty acid 7NS probing the pure sphingomyelin (□), cholesterol/sphingomyelin (1/1: mole/mole) (●) and 7-dehydrocholesterol/sphingomyelin (1/1: mole/mole) (◆).

proteins, viral proteins) could cluster and stabilize multiple microdomains [30].

The direct physical evidences for these domains remain relatively scarce in spite of their physiological relevance. The basic assumption is that the energy of the association of SM-CHOL exceeds that of the association of fluid GPL with CHOL at the physiological temperature. The domain stability over a long period of time requires that the lateral diffusion of CHOL between gel SM and the surrounding fluid GPL does not smear out the domains as rapidly as the mean lateral diffusion of lipids. X-Band (9–10 GHz) CW-ESR has an appropriate time-scale for the observation of the spin labeled lipid exchange dependent on the lateral diffusion rate in the order of 10^{-11} m^2 s [31–33]. Because fluorescence studies indicated that the dimension of the domains is extremely small (< 70 nm) in cell membranes [34], we suggest that microdomains represent a dynamic equilibrium between extended phase-separated domains and the intermixing of SM and CHOL within the fluid-surrounding matrix.

A quantitative investigation of the phase-heterogeneity by means of the *ensemble-average* parameter of spin-labeled fatty acids has been performed by means of spectral simulations. The main information provided by the simulation methods outlined here is the determination of the 'true' (or *ensemble-average*) parameter $\bar{P}_2$ from partially resolved two-component spectra or from spectra of probes reorienting slowly. The comparison of 16NS with 7NS reveals an unexpectedly low order parameter for 7NS. This is a further evidence for an exchange between ordered and disordered domains. The different behavior of 16NS and 7NS points out the narrowness of the experimental conditions where such an observation can be achieved. Phase-separation is not apparent in the presence of CHOL or DHCHOL whatever is the spin-labeled probe when the spectra are interpreted qualitatively. Only a quantitative interpretation based on computer simulation suggests that the heterogeneity has been averaged-out within the ESR time-scale by the highly enhanced mobility of the 16NS probe in the center of the lipid core in the presence of sterols

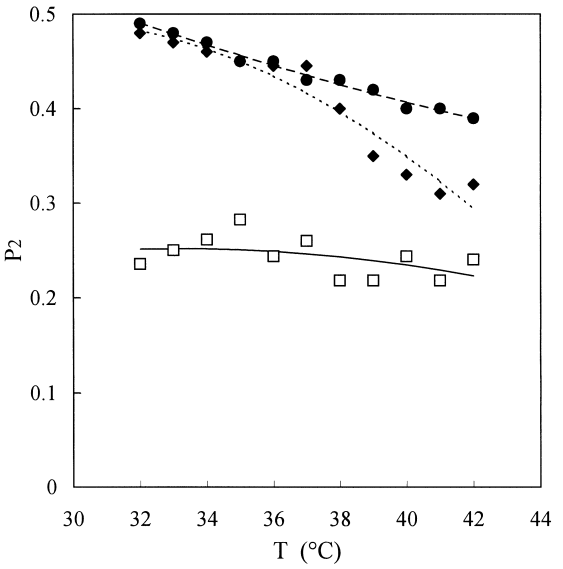

Fig. 6. Temperature dependence of the order parameter $\bar{P}_2$ of the spectrum of 7NS probing a mixture of sphingomyelin/phosphatidylethanolamine/phosphatidylserine before (□) and after addition of cholesterol (●) or 7-dehydrocholesterol (◆). The sterols are added in an equimolar ratio with SM.

(Table 1). A conclusion that the motion of 7NS probe is relevant to the slow-motion regime is not straightforward, but the difference recorded between CHOL and DHCHOL in the ternary lipid mixture at temperatures over 36°C reveals clearly the specific association of SM with CHOL. DHCHOL behaves like CHOL at the lowest temperatures investigated but the dissociation of the Lo phase formed by the former with SM occurs from 36°C whereas a stable Lo phase is formed with CHOL at least up to 42°C. Interestingly, the distinct behavior of CHOL and DHCHOL is revealed in a mixture of SM with a large fraction of amino-glycerophospholipids. The composition of this mixture is reminiscent of the inner leaflet of biological membranes where the microdomains are expected to be formed under the conditions of the cell physiology which includes an asymmetrical distribution of GPL between the two leaflets [35]. The present observation supports also the view that the substitution of CHOL by DHCHOL could change dramatically the membrane properties of embryonic cells affected by a deficit of the conversion of DHCHOL to CHOL as in the human Smith–Lemli–Opitz syndrome. At the physiological temperature the unstable association of SM/DHCHOL could compromise the association which forms the microdomains required for the activation of the developmental protein Sonic Hedgehog.

References

[1] K. Simons, E. Ikonen, Functional rafts in cell membranes, Nature 387 (1997) 569–572.

[2] R.E. Brown, Sphingolipid organization in biomembranes: what physical studies of model membranes reveal, J. Cell Sci. 111 (1998) 1–9.

[3] A.K. Batta, G.S. Tint, G. Salen, S. Shefer, M. Irons, E.R. Elias, Identification of 7-dehydrocholesterol and related sterols in patients with Smith–Lemli–Opitz syndrome, Genetics 50 (1994) 334.

[4] A. Rietveld, S. Neutz, K. Simons, S. Eaton, Association of sterol- and glycosylphosphatidylinositol-linked proteins with *Drosophila* raft lipid microdomains, J. Biol. Chem. 274 (1999) 12049–12054.

[5] B. Llirbat, C. Wolf, F. Chevy, D. Citadelle, G. Béréziat, Ch. Roux, Normal and inhibited cholesterol synthesis in the cultured rat embryo, J. Lipid Res. 38 (1997) 22–34.

[6] D. Chapman, N.F. Owens, M.C. Phillips, D.A. Walker, Mixed monolayers of phospholipids and cholesterol, Biochim. Biophys. Acta 183 (1969) 458–465.

[7] M.B. Sankaram, T.E. Thompson, Interaction of cholesterol with various glycerophospholipids and sphingomyelin, Biochemistry 29 (1990) 10670–10675.

[8] P.R. Maulik, G.G. Shipley, *N*-Palmitoyl sphingomyelin bilayers: structure and interactions with cholesterol and dipalmitoylphosphatidylcholine, Biochemistry 35 (1996) 8025–8034.

[9] S.N. Ahmed, D.A. Brown, E. London, On the origin of sphingolipid/cholesterol-rich detergent-insoluble cell membranes: physiological concentrations of cholesterol and sphingolipid induce formation of a detergent-insoluble, liquid-ordered lipid phase in model membranes, Biochemistry 36 (1997) 10944–10953.

[10] P. Mattjus, R. Bittman, C. Vilcheze, J.P. Slotte, Lateral domain formation in cholesterol/phospholipid monolayers as affected by the sterol side chain conformation, Biochim. Biophys. Acta 1240 (1995) 237–247.

[11] C. Wolf, C. Chachaty, H. Takahashi, I. Hatta, P.J. Quinn, Phase transition sequence between fluid liquid-crystalline and interdigitated lamellar gel phases in mixed-chain diacyl phosphatidylcholine, Chem. Phys. Lipids 87 (1997) 111–124.

[12] R. Brière, H. Lemaire, A. Rassat, Nitroxyde XV. Synthèse et étude de radicaux libres stables pipéridiniques et pyrrolidiniques, Bull. Soc. Chim. Fr. 35 (1965) 3273–3283.

[13] O.H. Griffiths, P.C. Jost, Lipid spin-labels in biological membranes, in: L.J. Berliner (Ed.), Spin Labeling Theory and Applications, vol. 1, Academic Press, New York, 1976, pp. 453–523.

[14] H.M. McConnell, Molecular motion in biological membranes [and Appendix A: Rotational correlation times, pp. 554–556], in: L.J. Berliner (Ed.), Spin Labeling Theory and Applications, vol. 1, Academic Press, New York, 1976, pp. 525–560.

[15] D.J. Schneider, J.H. Freed, Calculating slow motional magnetic resonance spectra. A user's guide, in: L.J. Berliner, J. Reuben (Eds.), Spin Labeling Theory and Applications, Biological Magnetic Resonance, vol. 8, Plenum Press, New York, 1989, pp. 1–76.

[16] D.E. Budil, L. Sanghyuk, S. Saxena, J.H. Freed, Non linear least-squares analysis of slow motion EPR spectra in one and two dimensions using a modified Levenberg–Marquardt algorithm, J. Magn. Res. Ser. A 120 (1996) 155–189.

[17] P.L. Nordio, General magnetic resonance theory and Linewidths parameters, in: L.J. Berliner (Ed.), Spin Labeling Theory and Applications, vol. 1, Academic Press, New York, 1976, pp. 1–52.

[18] J.H. Freed, Stochastic-molecular theory of spin relaxation for liquid crystals, J. Chem. Phys. 66 (1977) 4183–4199.

[19] P. Jost, L.J. Libertini, V.C. Hebert, O.H. Griffith, Lipid

spin-labels in lecithin multilayers. A study of motion along fatty acid chains, J. Mol. Biol. 59 (1971) 77–98.
[20] D.W Marquardt, An algorithm for least-squares estimation of non-linear parameters, J. Soc. Ind. Appl. Math. 11 (1963) 431–441.
[21] C. Chachaty, E.J. Soulié, Determination of electron spin resonance static and dynamic parameters by automated fitting of the spectra, J. Phys. III France 5 (1995) 1927–1952.
[22] J. Davoust, P.F. Devaux, Simulation of electron spin resonance spectra of spin-labeled fatty acids covalently attached to the boundary of an intrinsic membrane protein. A chemical exchange model, J. Magn. Res. 48 (1982) 475–494.
[23] D. Marsh, Experimental methods in spin-label spectral analysis and two-site exchange simulation, in: L.J. Berliner, J. Reuben (Eds.), Spin Labeling Theory and Applications, Biological Magnetic Resonance, vol. 8, Plenum Press, New York, 1989, pp. 255–303.
[24] W.L. Hubbell, H.M. McConnell, Molecular motions of spin-labeled phospholipids and membranes, J. Am. Chem. Soc. 93 (1971) 314–326.
[25] M.B. Sankaram, T.E. Thompson, Interactions of cholesterol with various glycerophospholipids and sphingomyelin, Biochemistry 29 (1990) 10670–10675.
[26] M.B. Sankaram, T.E. Thompson, Cholesterol-induced fluid-phase immiscibility in membranes, Proc. Natl. Acad. Sci. USA 88 (1991) 8686–8690.
[27] J.M. Smaby, H.L. Brockman, R.E. Brown, Cholesterol's interfacial interactions with sphingomyelins and phosphatidylcholines: hydrocarbon chain structure determines the magnitude of condensation, Biochemistry 33 (1994) 9135–9142.
[28] R. Bittman, C.R. Kasireddy, P. Mattjus, J.P. Slotte, Interaction of cholesterol with sphingomyelin in monolayers and vesicles, Biochemistry 33 (1994) 11776–11781.
[29] R.J. Schroeder, S.N. Ahmed, Y. Zhu, E. London, D.A. Brown, Cholesterol and sphingolipid enhance the Triton X-100 insolubility of glycosylphosphatidylinositol-anchored proteins by promoting the formation of detergent-insoluble ordered membrane domains, J. Biol. Chem. 273 (1998) 1150–1157.
[30] D.A. Brown, E. London, Structure and origin of ordered lipid domains in biological membranes, J. Membrane Biol. 164 (1998) 103–114.
[31] P. Devaux, H.M. Mc Connell, Lateral diffusion in spin labeled phosphatidylcholine, J. Am. Chem. Soc. 94 (1972) 4475–4481.
[32] P. Devaux, C.J. Scandella, H.M. McConnell, Spin–spin interactions between spin labeled phospholipids incorporated into membranes, J. Magn. Reson. 9 (1973) 474–485.
[33] M. Bloom, J.L. Thewalt, Time- and distance-scales of membrane domain organization, Molec. Membrane Biol. 12 (1995) 9–13.
[34] R. Varma, S. Mayor, GPI-anchored proteins are organized in submicron domains at the cell surface, Nature 394 (1998) 798–801.
[35] E.M. Bevers, P. Comfurius, D.W.C. Dekkers, R.F.A. Zwaal, Lipid translocation across the plasma membrane of mammalian cells, Biochim. Biophys. Acta 1439, 317–330.